Article

A Study on the Effect of Green Plot Ratio (GPR) on Urban Heat Island Intensity and Outdoor Thermal Comfort in Residential Areas

Jian Zheng [1], Zilong Li [2,*] and Bohong Zheng [2,*]

1   School of Architecture, Changsha University of Science and Technology, Changsha 410076, China; zhengjian@csust.edu.cn
2   School of Architecture and Art, Central South University, Changsha 410075, China
*   Correspondence: 221312024@csu.edu.cn (Z.L.); 203126@csu.edu.cn (B.Z.); Tel.: +86-178-7237-4349 (Z.L.); +86-138-7598-2310 (B.Z.)

Abstract: Greenery impacts the urban thermal environment, but the benefits of the three-dimensional green volume of space have not been effectively evaluated. In this paper, we analyzed the impact of 3D greenery on urban heat island intensity and thermal comfort in residential areas from the perspective of the green plot ratio (GPR). We selected a typical residential area, set up simulation models, and then analyzed the effect of different GPR values on the outdoor thermal environment using the validated ENVI-MET simulation. The results showed that increasing GPR in residential areas can effectively reduce the intensity of urban heat island and improve thermal comfort. When the GPR reaches 0.5 and 1.5, the thermal comfort level of the building overhead space and the north–south street space decreases from "very strong thermal stress" to "strong thermal stress". When the GPR reaches 2.5, the outdoor thermal comfort of the east–west street space and courtyard space is reduced to "hot". When the GPR is higher than 0.5, the urban heat island intensity in the north–south street space decreases by one level, from "very strong" to "strong". When the GPR reaches 3.5, all four types of spaces have "moderate" urban heat island intensity. Increased GPR exacerbates urban heat island intensity to some extent and worsens outdoor thermal comfort due to the nocturnal insulating effect of plants. Based on the results, the study proposes the bottom-line control of the GPR index from the perspective of urban heat island mitigation and thermal comfort improvement. This paper points out the benefits of GPR in residential areas in improving the human environment, which is of great practical value for developing urban residential environment from "increasing quantity" to "improving quality".

Keywords: green plot ratio; residential areas; urban heat island; thermal comfort; ENVI-MET

1. Introduction

1.1. The Necessity of Greenery in Residential Areas

As urbanization continues to increase, the construction of a healthy and livable urban environment is an essential element of future urban development [1–3]. However, rapid urbanization makes cities hotter than surrounding suburbs, affecting the urban thermal environment and threatening the health of urban residents [4]. In urban space, residential areas are the most relevant to the life and leisure of urban residents, and at the same time, they are the places where residents are most exposed to the outdoors [5]. As an important part of the urban ecosystem, residential greenery plays a vital role in regulating the urban climate, improving urban air quality, mitigating urban noise, improving urban landscapes, and increasing the thermal comfort of urban residents [6–8]. The urban residential area is a vital carrier with one of the four primary functions of the city (residence, work, recreation, and transport) [9]. Therefore, it is essential to clarify the relationship between greenery in residential areas and urban heat island intensity and outdoor thermal comfort. This is

vital for improving the urban thermal environment and promoting the physical and mental health of urban residents.

1.2. Current Research Perspectives on Greenery in Residential Areas

Plants, as the main component of greenery in residential areas, have a cooling and humidifying effect on the surrounding environment through transpiration [10]. Trees improve outdoor thermal comfort by lowering temperatures through canopy shading and transpiration [11]. Current studies, mainly qualitative and quantitative, have examined the impact of residential greenery on the outdoor thermal environment. From the qualitative perspective, this includes plant species and greenery layout. Firstly, different types of plants affect the thermal environment differently. A study in Shanghai, China, suggests that deciduous plants can effectively improve year-round thermal comfort in hot-summer and cold-winter climate by reducing excessive outdoor shading in winter compared with evergreen plants [12]. Trees have a more apparent cooling effect than grasses because they provide more shade and effectively intercept more solar radiation [13]. Of the three plant types, trees, shrubs, and grasses, trees are more effective than shrubs in improving thermal comfort, and shrubs are better than grasses [14]. The differences in the characteristics of the different types of trees resulted in apparent differences in their impact on the microclimate of the settlements [15]. Secondly, greenery layout and green space structure have a specific regulatory effect on the thermal environment. In terms of greenery layout, a green space surrounded by trees provides optimal thermal comfort for activities; the thermal comfort under both greenery layout structures of trees surrounded by shrubs and shrubs surrounded by trees is better than that of a single shrub [8]. A study comparing 17 tree layouts in a hot-summer and cold-winter climate zone noted that evenly dispersed trees provided a limited increase in shade from 11% to 14% but did not improve thermal comfort [16]. Tree species and planting spacing have an effect on the outdoor thermal environment. It was found that reducing the planting spacing of trees can improve thermal comfort to a certain extent and that trees with high leaf area density have a more apparent effect on the outdoor thermal environment [17]. Compared to bare ground or asphalt, grass can effectively reduce ground temperatures and the surface temperatures of neighboring buildings [18]. There were distinct differences in the cooling of different greenery layouts, and among the shrub–grass, arbor–grass, and arbor–shrub–grass greenery layouts, arbor–shrub–grass had the most apparent cooling effect on the region as a whole [19].

From a quantitative perspective, green space ratio, green coverage, and tree canopy coverage are commonly used to measure the quality of urban green spaces. The green space ratio is the percentage of green plants and does not take into account the vertical projection of trees, whereas green coverage and tree canopy coverage take it into account. Many studies have explored the effects of these indicators on the thermal environment. Urban green space can reduce surface temperature by reducing incident radiation through shading and dissipating heat through evaporation, so increasing the green space ratio obviously mitigates the urban heat island effect in urban residential areas [20]. By constructing scenarios with different green space ratio, it was shown that increasing the green space ratio can effectively improve outdoor thermal comfort in semi-arid climates [21]. In the tropical city of Singapore, increasing green coverage reduces the UTCI by about 3.0 °C at midday, but continued increase in green coverage leads to an increase in relative humidity, resulting in no sustained reduction in thermal comfort [22]. Increased tree canopy coverage effectively reduced air temperature and mean radiant temperature in urban residence, with air temperature and mean radiant temperature with high tree canopy coverage reduced by 3.3 °C and 13.9 °C, respectively, compared to urban residence with no tree canopy coverage [23]. A study in Nigeria showed that outdoor air temperature could be reduced by up to 3.38 °C and mean radiant temperature by up to 24.24 °C when 45 percent of the canopy was covered with trees [24]. Based on the consideration of thermal dynamics and human thermal comfort, the study quantified the maximum effective canopy cover thresholds of 45 percent, 30 percent, and 25 percent for residential areas of 33 m (11 floors),

54 m (18 floors), and 100 m (33 floors) in height, respectively [25]. Additionally, increased plant canopy density can intercept more solar radiation, reducing outdoor air temperature in residential areas and improving thermal comfort [26]. Increasing tree canopy coverage can provide a more comfortable thermal environment for the area compared to increasing the green space ratio [22]. Studies on the thermal environment of subtropical settlements have found that even in neighborhoods with a high green space ratio, the maximum outdoor temperature can be up to 34 °C, and the total horizontal solar radiation intensity can be up to 1000 W/m² [27]. Actually, the green space ratio, green coverage, and tree canopy coverage quantify the rate of plant coverage per unit area. These indicators are only considered from the perspective of the horizontal surface but cannot reflect the actual three-dimensional green volume of plants. The three-dimensional green volume reveals the spatial volume of plants through the calculation of stem and leaf volume [28]. As a greenery index, it breaks through the limitations of the original two-dimensional greenery index and can more accurately reflect the reasonableness of the plant composition of the residential area. A synthesis of existing research results reveals fewer articles analyzing and evaluating the impact of greenery on the thermal environment of residential areas from the perspective of three-dimensional greenery, and there is a noticeable gap in research in this area.

1.3. A New Perspective on Measuring Plants Eco-Efficiency Using Green Plot Ratio (GPR)

To fill the gaps in the existing research referred to, related scholars have defined the green plot ratio (GPR) to measure the three-dimensional green volume of plants by combining the concept of building plot ratio (BPR, total building area divided by the building site area) in the field of urban planning. The GPR is calculated by drawing on the BPR method and introducing the leaf area index (LAI) of plants, that is, the total plant leaf area per unit of land [29]. The GPR can be obtained by calculating the overall amount of plant greenery in the area, thus enabling the assessment and control of green space quality. China's current design standards related to residential areas contain provisions for greenery in residential areas. The Urban Residential Planning and Design Standards states that the green space ratio in new urban areas should be no less than 30% and that the ratio for the reconstruction of old cities should be no less than 25% [30]. However, the outdoor space of many residential areas only meets the lower limit of the green space ratio indicator in the construction process in practice [31], which leads to a reduction in the quality of the outdoor space and a deterioration of the thermal environment [32]. Design standard for green building in Hunan province points out that the combination of trees, shrubs, and grasses should be used in a compound greenery way, and the green space should not be planted with less than 3 trees/100 m² to reduce the intensity of urban heat island [33]. In Jiangsu Province, China, the ratio of the canopy projection area of trees and shrubs to the lawn area should not be less than 4:1 [34]. Design standard for residential buildings in Sichuan Province states that the green plot ratio is the ratio of the total leaf area of various types of vegetation in the site (minus the building base area) to the site area, and stipulates that the GPR of the site in the residential area should not be less than 3.0 [35]. In Shenzhen, Shanghai and Fujian [36–38], the site GPR shall not be lower than 3.0. The above standards indicate that the evaluation standard of urban green space quality is developed from the traditional two-dimensional indexes, such as green space ratio and green coverage, to the three-dimensional indexes represented by GPR, and the benefits of urban green space will be analyzed more comprehensively. However, the current research has not been able to analyze the impact of GPR on the thermal environment of the residential area, and there are fewer studies on the measurement and simulation of the GPR as an evaluation index. Therefore, it is necessary to analyze the influence of GPR on the outdoor thermal environment.

1.4. Scientific Hypothesis and the Sub-Goals

From the above analysis, we realize a scientific question. GPR, as an indicator that is gradually being emphasized, we have paid little attention to its impact on the thermal environment of residential areas. Although GPR is required in some areas, we still do not know the effect of different values of GPR on the outdoor thermal environment, whether raising GPR all the time always has a positive effect, and if not, whether there is a lower or upper limit. These indicate that there is still a gap. Therefore, we conducted this study and proposed the following objectives.

Firstly, a research framework was established (shown in Figure 1), which briefly describes the main steps of this study. It is worth noting that this is applicable to specific climate zones and can be extended to more climate zones.
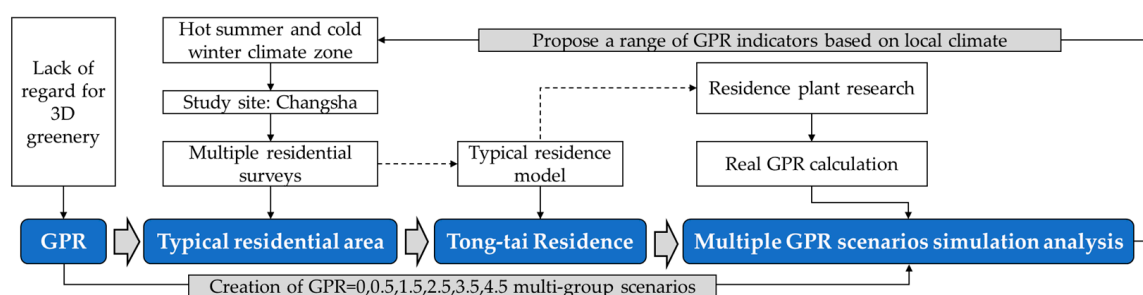

Figure 1. Research framework.

Secondly, we study the effects of different GPR values on the urban heat island effect and thermal comfort in residential areas and explore the relationship between GPR values and urban heat island intensity and thermal comfort. Based on the results, a reasonable range of GPR values is proposed.

Finally, we call on scholars in more countries or regions to emphasize the impact and benefits of GPR to help new urban development planning to cope with climate warming and thermal environmental degradation.

In the following sections, we took a residential area in a hot-summer and cold-winter climate zone as the research object and adopted the combination of field observation and numerical simulation. We took the GPR as the evaluation index, established the regional GPR scenario, and constructed the ENVI-MET model from the effect of different GPR values on the urban heat island intensity and thermal comfort in the residential area. This research aims to provide scientific guidance and suggestions for the greenery planning of residential areas to alleviate the urban heat island effect and improve the thermal comfort of residents.

2. Materials and Methods

2.1. Study Site and Typical Residential Area

The study site is located in Changsha, Hunan Province, China. Changsha is a typical subtropical monsoon climate zone [39], and meanwhile belongs to the hot-summer and cold-winter zone in China's building climate zones [40]. The average daily air temperature from June to September can reach over 25 °C, and there are nearly 84 days with an average daily temperature greater than 30 °C. Winter is cold, and the severe cold period below 0 °C is relatively short [41,42]. Changsha has high humidity, with the average annual precipitation reaching 1472.9 mm. Spring is cloudy and rainy, with very heavy precipitation; summer precipitation is uneven, with stormy weather mainly concentrated from May to June; autumn has little precipitation and mostly sunny weather with suitable temperatures; and winter precipitation accounts for 16% of the year [43].

Based on the introduction of the study site, we further analyzed the residential area. In this study, we introduced the concept of a typical residential area. It can be understood as a prototype similar to or close to most residences within a region. This is mainly in

terms of spatial morphology and relevant settlement indicators. In order to understand the characteristics and indicators of Changsha's residential spatial morphology, we selected a number of residential areas for analysis based on field research, as shown in Figure 2. Firstly, we analyzed from the point of view of the residence plot area. Among the selected research samples, the number of residence plot area distribution of 4~4.5 hm^2 is the largest, which is 32%. Secondly, the shape of residential plots is affected by natural conditions, social and historical development, economic development mechanisms, and other factors, resulting in different plot shapes on the plane [44]. By analyzing the aspect ratios of the plots in the sample, it can be seen that the total proportion of residential areas with aspect ratios of 0.75~1.0 and 1.0~1.5 is 72%, meaning that residential plots are mostly rectangular. Analyzed from the perspective of the orientation of residential plots, the proportion of residential plots with a declination angle of $\pm 5.4°$ in the samples is 60%, indicating that the orientation of Changsha's residential areas is primarily due south and north. The architectural layout of the residential areas in the sample mainly includes row-type, enclosed-type, and mixed-type (point-type + row-type). Among them, the proportion of row layout is 65.8%, and the proportion of enclosed layout is 7.9%. It can be seen that Changsha's residential buildings are dominated mainly by row and column layouts. The number of floors of residential areas in the statistical samples belongs to the multi-story and high-rise category. Multi-story category I accounts for 23.7%, multi-story category II accounts for 10.5%, high-rise category I accounts for 47.4%, and high-rise category II accounts for 13.2%, of which high-rise category I (10~18 floors) accounts for the largest proportion. Additionally, the proportion of residential areas with a building density of 25% or less in the sample was 60.5%.
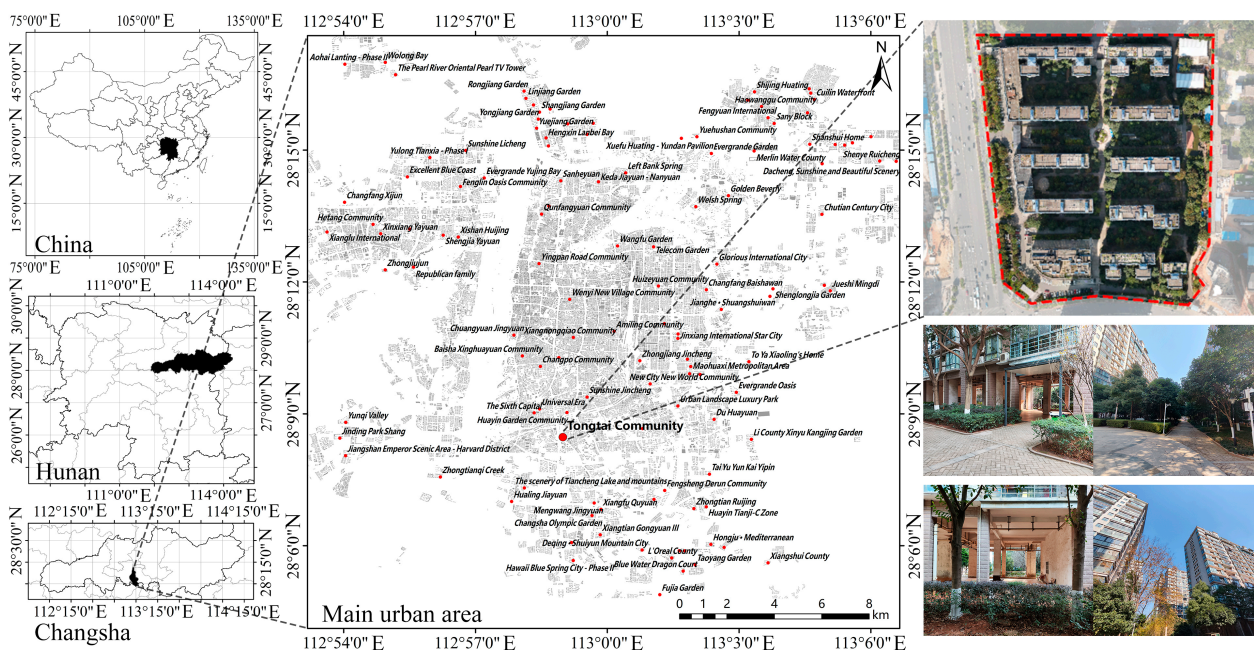

Figure 2. Residential area research and selection of research subjects, red dotted box represent residential areas.

Based on the above analysis, we selected the Tong-tai residence in the Tian-Xin District of Changsha City, China, as the typical residential area for the measurements and simulations. The typical residential area is located in the city center of Changsha (112°58′ E, 28°11′ N, 23.5 m above sea level), Hunan, China (Figure 2). From the aspects of spatial morphology and relevant indicators of the settlement, the land area of the residential area is about 4.43 hectares. The overall shape of the plot is regular, consisting of ten 14 floors (high-rise category I) residential buildings, with a building density of about 23.9%, and the buildings are arranged in rows and columns, facing south and north; the buildings on the north and south sides jointly enclose to form the space of the street, and the height-to-width

ratio of the street is about 1.75. Concrete pavements, broadleaf trees, shrubs, and grasses are uniformly distributed in the street space, forming the lower bedding surface of the residential area. Based on the area of the residence, building layout form, building height, building density and other indicators, we believe that the Tong-tai residence is typical.

2.2. Calculation of GPR and Modeling of Six Scenarios

Green plot ratio (GPR) is a widely used indicator to quantify the three-dimensional green volume of green space. In 2003, a Singaporean scholar proposed the planning index of green plot ratio (GPR) based on the biological parameter leaf area index (LAI), defined as the average green area of a plot of land, which is the average of the green area of a site [29]. The leaf area index (LAI) can be used to measure the structural type of green space. The higher the value of LAI, the larger the total leaf area of plants per unit area and the richer the type of vegetation structure. The concept of building plot ratio is borrowed in the evaluation of urban green space, and GPR is defined as the green plot ratio, which is the total plant leaf area per unit of land. The formulas are shown in (1) and (2). We conducted field counts of five species of trees, one shrub, and one grass that dominate the residential area, and the counts are shown in Table 1. According to the formulas, we calculated the GPR for Tong-tai residence to be 3.43, which is close to 3.5.

$$GPR = LA/S \tag{1}$$

$$GPR = \frac{\sum_a N_a \cdot \pi R_a^2 \cdot LAI_a + \sum_b N_b \cdot \pi R_b^2 \cdot LAI_b + \sum_c S_c \cdot LAI_c}{TA} \tag{2}$$

where LAI represents the sum of leaf area in a given region, and S represents the total land area of the region. N_a is the number of trees (a), R_a is the canopy radius of trees (a), and LAI_a is the leaf area index of trees (a); N_b is the number of shrubs (b), R_b is the radius of shrubs (b), and LAI_b is the leaf area index of shrubs (b); S_c is the area covered by grass (c), and LAI_c is the leaf area index of grass (c). TA represents the total land area of the study area.

Table 1. Number or area of plants counted in the field.

Plants Name	Total Number or Total Area
Michelia maudiae Dunn.	121 trees
Koelreuteria bipinnata Franch.	67 trees
Cinnamomum camphora (L.) Presl.	76 trees
Prunus subg. *Cerasus* sp.	127 trees
Osmanthus sp.	140 trees
Camellia japonica L.	63 trees
Reineckea carnea (*Andrews*) Kunth	12,800 m^2

According to the GPR formulas, we can adjust the number of plants to construct different GPR scenarios. In order to facilitate the subsequent ENVI-MET modeling, we selected the above plants as the representative plants of the plot's greenery. Table 2 shows the total number of trees in different GPR scenarios. In addition to trees and shrubs, we used grass as a fixed quantity. When GPR = 0, there is no vegetation on the site. The size and amount of grass are the same in the other five scenarios.

Figure 3 illustrates the six GPR scenarios established by the study. At GPR = 0, there is no vegetation in the residence. This scenario is mainly used as a comparison to analyze the cooling and thermal comfort improvement effects of greenery. The number of plants on the site gradually increased as the GPR increased to 0.5, 1.5, 2.5, 3.5, and 4.5, and the increase in plants followed a randomized layout. We chose GPR = 4.5 as the upper limit because in the actual greenery layout of residential areas, few residential areas can be planted with such a large number of plants due to economic considerations. This study focuses on the

effect of varying the value of GPR between 0 and 4.5 on the thermal environment of a residential area.

Table 2. Total number of trees for different GPR scenarios.

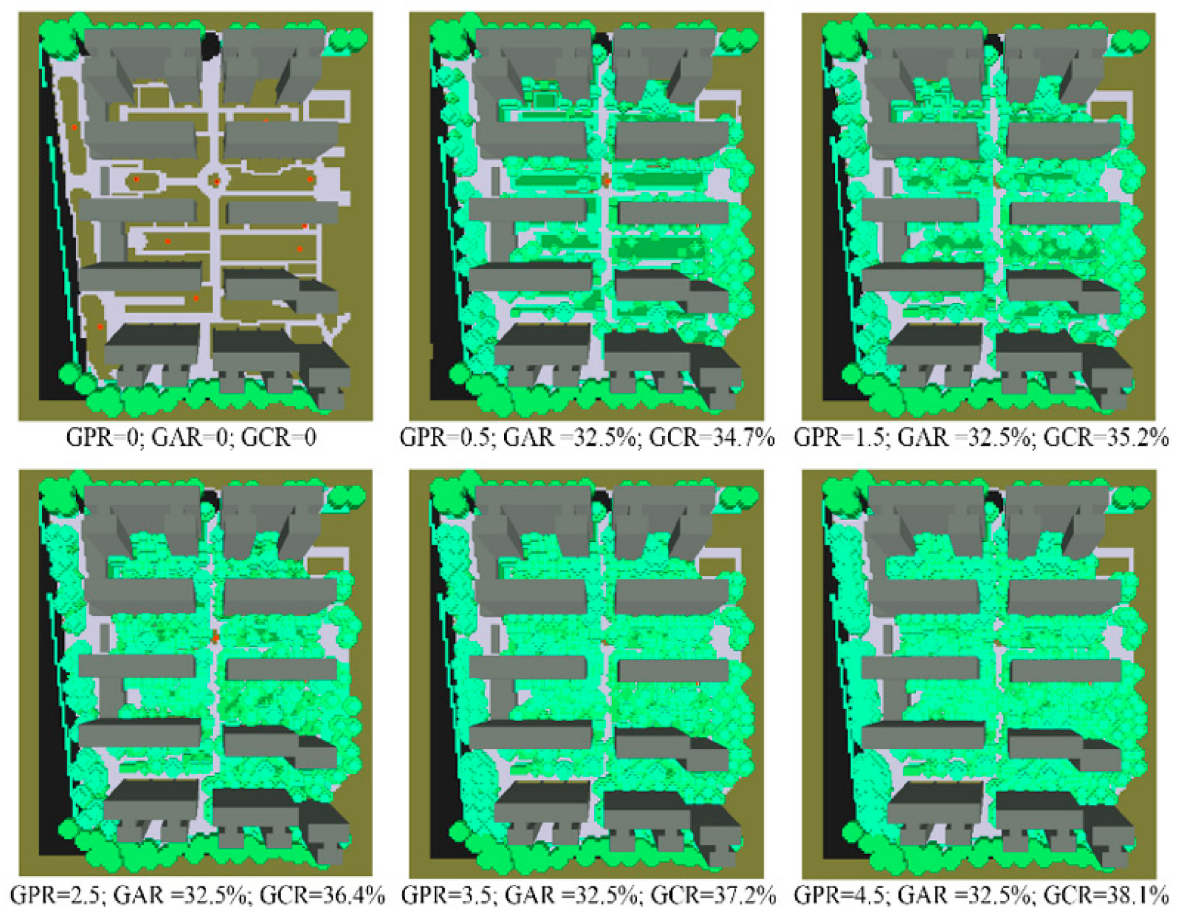| Different GPR Scenarios	Total Number of Trees
GPR = 0	0
GPR = 0.5	113
GPR = 1.5	229
GPR = 2.5	435
GPR = 3.5	610
GPR = 4.5	860

Figure 3. Aerial view of the ideal model and parameter indicators, GPR represents green plot ratio, GAR represents green area ratio, and GCR represents green coverage ratio.

2.3. Measurement and Accuracy Verification

On-site measurement is one of the essential ways to evaluate the characteristics of the thermal environment objectively, and at the same time, it is an essential basis for verifying the accuracy of numerical simulation. In the study, a typical weather day in summer was selected for the field measurement, and the air temperature (Ta), relative humidity (RH), black globe temperature (Tg), and wind speed (Va) at 1.5 m near the ground were measured by different testing instruments. Finally, the open-source software Rayman 1.2 was used to calculate the thermal comfort indicators mean radiant temperature (Tmrt) and physiological equivalent temperature (PET). The study focused on the microclimate distribution at pedestrian heights, so the experimental instruments were arranged at 1.5 m above the ground. The study area was surveyed, and the green points in Figure 4 are

DS1923 (i-Button) temperature and humidity data recorders, with a total of 10 groups; the blue points are hand-held temperature and humidity recorders, with a total of 12 groups; and the red points were Kestrel 5500 meteorological instrument, with a total of 3 groups. DS1923 (i-Button) were mainly arranged in the green group of the residential area. The Kestrel 5500 meteorological instruments were located at the entrance square on the west side of the residential area, the central square, and the first elevated floor of the residential area. Table 3 describes the metrics associated with the measurement instruments.

Figure 4. Layout of survey points and related instrumentation in the study area.

**Table 3.** Introduction to the relevant indicators of measuring instruments.

Measuring Instruments	Measurement Indicators	Measurement Range	Instrument Precision	Range of Error
JANTYTHCH 2022	air temperature	−20~100 °C	0.1 °C	±0.5 °C
	wind speed	0~10 m/s	0.1 m/s	±0.5 m/s
	black globe temperature	−20~100 °C	0.1 °C	±0.5 °C
Kestrel 5500	wind direction	0~360°	1°	±3°
	wind speed	0~70 m/s	0.1 m/s	±0.5 m/s
DS1923 (i-Button)	Ta/RH	−40~80 °C/0%~100%	0.1 °C/0.1%	±0.3 °C/±0.5%

The parameter settings for the study validation simulation are shown in Table 4, including geographic location, simulation time, and meteorological parameters.

Table 4. ENVI-MET simulation parameter settings.

Simulation Parameters	Settings
Geographic location	Changsha (28.11° N, 112.58° E)
Simulation time	Date: 7 August 2021 Start time: 2:00 Duration of simulation: 32 h
Meteorological parameters	Minimum air temperature 28.7 °C Maximum air temperature 34.45 °C
	Maximum humidity: 87.66% Minimum humidity 59.75%
	Wind speed: 2.0 m/s
	Wind direction: 180°

Comparing the measured and simulated values, the correlation coefficients of air temperature, mean radiant temperature, and physiological equivalent temperature were 0.833, 0.825 and 0.809, respectively (Figure 5). Since the R^2 is closer to one, the measured data fits the simulated data better, and the measured and simulated values in the present study have an obvious correlation and a high degree of fit. It could be seen that the simulation of ENVI-MET on thermal environment parameters is effective, and its simulated values are highly fitted to the measured values.

(a) (b) (c)
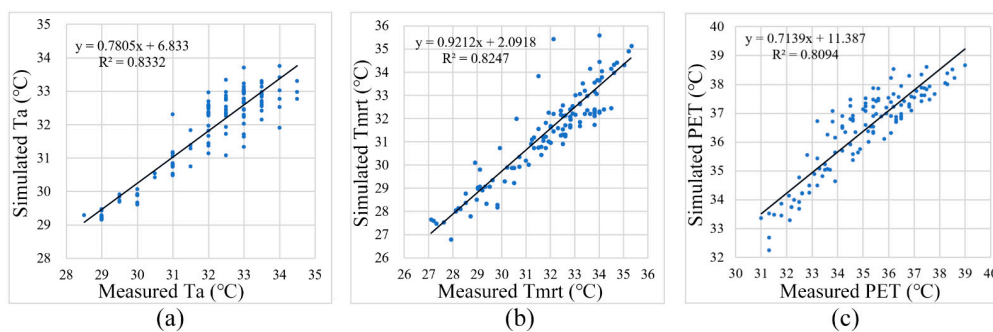
Figure 5. Comparison of measured and simulated values of air temperature (**a**), mean radiant temperature (**b**), and physiological equivalent temperature (**c**) in the study area.

In order to quantify the difference between the measured and simulated data, we used the root mean square error (RMSE), mean absolute error (MAE), and mean absolute percentage error (MAPE) to evaluate the results and reflect the accuracy and applicability of the model with the following formulas. Among them, it is generally believed that the MAPE value is less than 10%, indicating that the simulation prediction accuracy is high; the smaller the values of RMSE and MAE, the higher the accuracy of the simulation results. Moreover, some scholars have found that the RMSE of ENVI-MET simulated values and measured values are approximately between 0.66 and 7.98 °C, and it is currently believed that the RMSE is approximately between 0.52 and 4.30 °C [45], and MAE approximately between 0.27 and 3.67 °C is acceptable.

$$\text{RMSE} = \sqrt{\frac{1}{m}\sum_{i=1}^{m}(Y_{obs,i} - Y_{model,i})^2} \tag{3}$$

$$\text{MAE} = \frac{1}{m}\sum_{i=1}^{m}\left|(Y_{obs,i} - Y_{model,i})\right| \tag{4}$$

$$\text{MAPE} = \frac{1}{m}\sum_{i=1}^{m}\frac{\left|Y_{obs,i} - Y_{model,i}\right|}{Y_{obs,i}} \times 100\% \tag{5}$$

In the formula, RMSE is the root mean square error; MAE is the mean absolute error; MAPE is the mean absolute percentage error; Y_{obs} is the measured value; Y_{model} is the simulated value; m is the number of data samples; and i is the number of samples, i = 1, 2, 3 ...m.

In Table 5, root mean square error (RMSE), mean absolute error (MAE), and mean absolute percentage error (MAPE) evaluations were performed and analyzed for air temperature, mean radiant temperature, and physiological equivalent temperature in the study area. It can be found that the RMSE, MAE, and MAPE of air temperature in the study area are 0.643, 0.484, and 1.48%, respectively; the RMSE, MAE, and MAPE of mean radiation temperature are 0.970, 0.746, and 2.32%, respectively; and the RMSE, MAE, and MAPE of physiological equivalent temperature are 1.600, 1.387, and 4.04%, respectively.

Table 5. RMSE, MAE, and MAPE of measured and simulated values at monitoring points.

Indicators	Ta	Tmrt	PET
RMSE	0.64 °C	0.97 °C	1.60 °C
MAE	0.48 °C	0.75 °C	1.39 °C
MAPE	1.48%	2.32%	4.04%

The error evaluation metrics, i.e., RMSE value, MAE value, and MAPE value, of all the above-mentioned thermal environment metrics are within the permissible range, indicating that the error between measured and simulated values in this study is small. In this study, the air temperature error is the smallest, the mean radiant temperature is the second largest, and the physiological equivalent temperature error is the last. This is related to the fact that the simulation environment established in ENVI-MET is relatively simple, and the simulation results are more ideal compared with the measured results; in the measured environment, the urban construction environment is more complicated, and the air temperature, relative humidity, wind speed, etc., are easily affected by the surrounding environment and human activities, and the calculation of the physiological equivalent temperature and the mean radiant temperature involves several microclimate parameters; in addition, the data obtained in the actual measurement are instantaneous, and the data obtained in ENVI-MET's simulation are the most accurate. In addition, the data obtained in actual measurements are instantaneous values, while the ENVI-MET simulation environment is set to continuous values. Additionally, for this study, the authors analyzed the stability of the ENVI-MET software 5.0 to ensure the reliability of the results. Based on the existing research results and the calibration experiments in this study, it is still a reliable scientific tool to study the outdoor thermal environment in hot-summer and cold-winter zone, with good modeling accuracy. It can predict the microclimate environment of the study area.

2.4. Data Extraction Point Layout and Data Analysis

In order to comprehensively assess the impact of GPR on outdoor spaces in residential areas, the study categorizes outdoor spaces into street space, courtyard space, and building overhead space based on the function of the space. Street space includes the primary and secondary roads in the residential area, a space with obvious transportation attributes, and is divided into east–west street space and north–south street space in this study. Courtyard space includes enclosed and semi-enclosed courtyards, which are enclosed by buildings with weak openness. Building overhead space refers to the open space layer of a building that is supported only by structural columns without enclosing walls, and it is a semi-indoor, public gray space that is well connected to the outside. For the data extraction of each space, the study refers to the established methods and follows the principle of uniform layout of extraction points to ensure the science and rationality of the extracted data. The layout of data extraction points is shown in Figure 6. Additionally, to investigate the effect of GPR on the thermal environment of the residential area further, the study will analyze

the daytime and nighttime hours separately. In contrast to the daytime hours, the nighttime hours are free of solar radiation, and the ground scattering effect dominates.
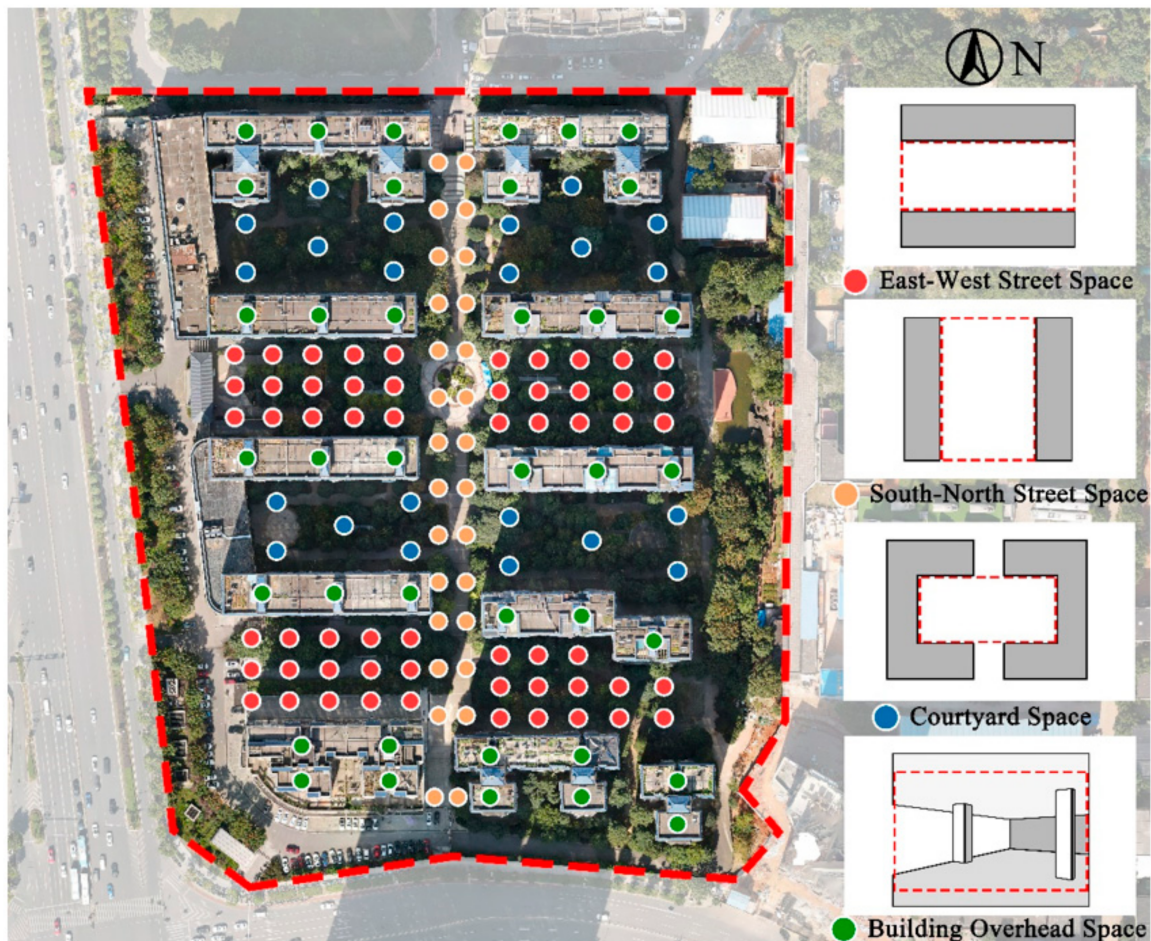

Figure 6. Layout of simulated data extraction points.

The study extracted data for the air temperature and PET at the pedestrian height of 1.5 m and calculated the urban heat island intensity, which is the difference between the mean air temperature in the city center and the mean air temperature in the surrounding suburbs (countryside). Physiological equivalent temperature (PET) was chosen to quantify thermal comfort. Physiological equivalent temperature integrates air temperature, humidity, wind speed, solar radiation, clothing, and exercise. It is the most accurate and widely used, and its scientific validity has been proved by domestic and international scholars' research [46].

3. Results

3.1. Impact of GPR on Urban Heat Island Intensity in Residential Areas

3.1.1. Impact of GPR on Urban Heat Island Intensity during Daytime

The urban heat island intensity of the residential space is mitigated to varying degrees as the GPR increases. In Figure 7, the urban heat island intensity mitigation occurred in the east–west street space during the GPR increase from 0 to 4.5, with the urban heat island intensity decreasing from 3.91 °C to 2.89 °C. The urban heat island intensity of the north–south street space is reduced by 0.90 °C. The urban heat island mitigation effect of the courtyard space and the building overhead space is the same, with the urban heat island intensity reduced by 0.95 °C and 0.94 °C, respectively. For the north–south street space, the GPR increase from 3.5 to 4.5 still mitigates urban heat island intensity by up to 0.12 °C. However, the GPR increase does not consistently mitigate urban heat island

intensity for the other types of spaces. In the courtyard space, the GPR increased from 3.5 to 4.5, with only a 0.02 °C reduction in urban heat island intensity, a 0.04 °C reduction in urban heat island intensity in the east–west street space, and a 0.05 °C reduction in the building overhead space. Figure 8 shows the outdoor air temperature distribution in the residential space at 14:00.
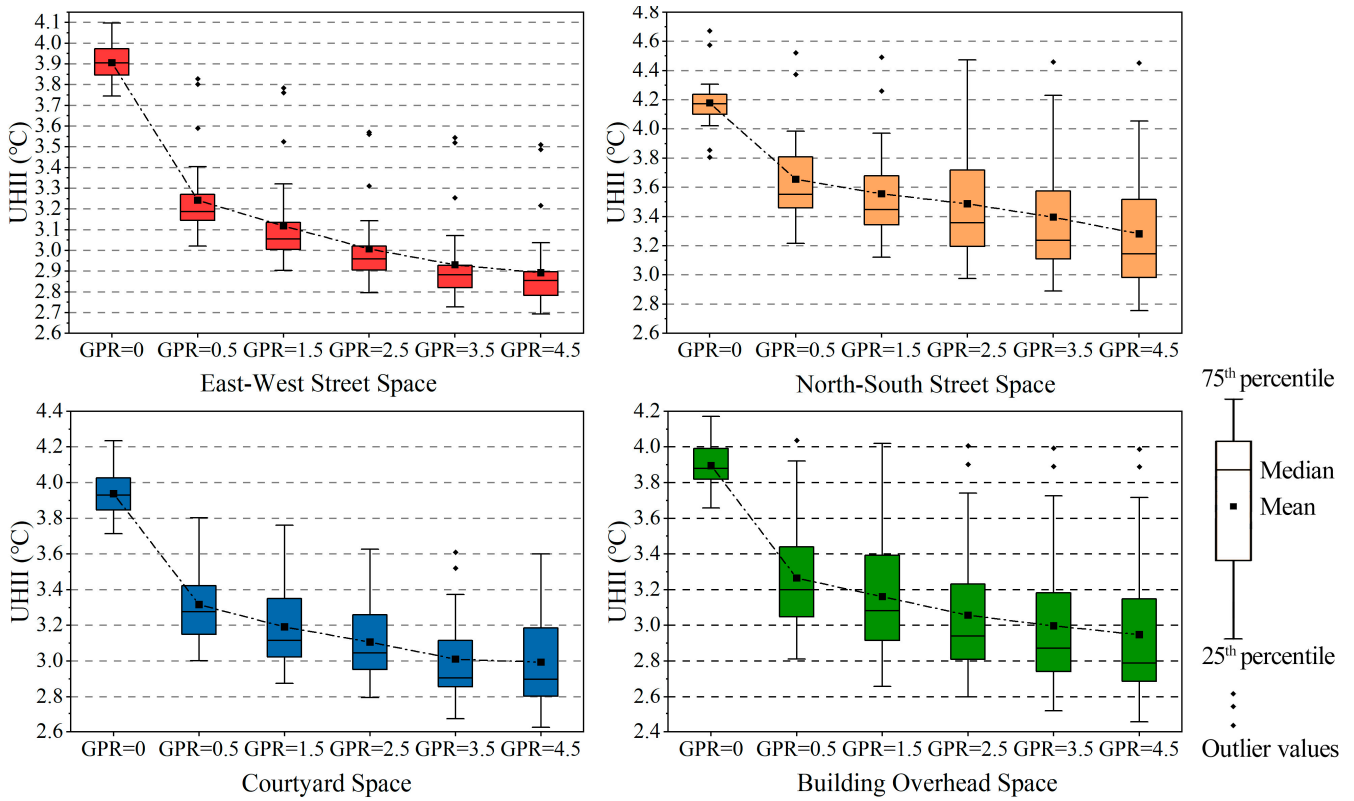

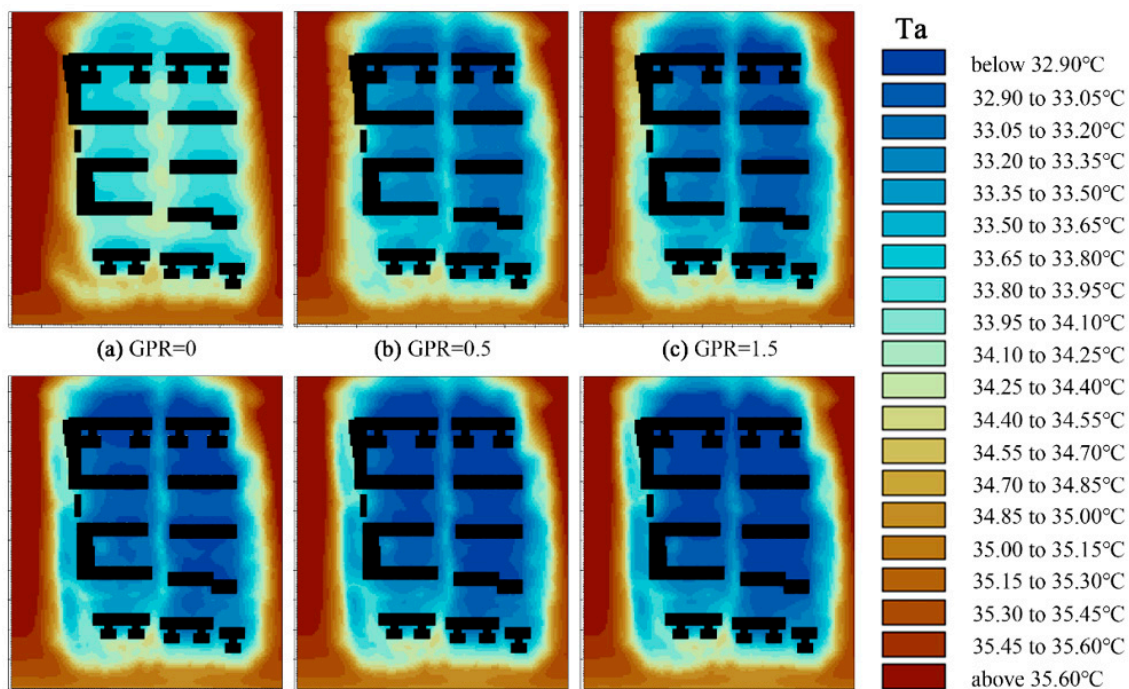**Figure 7.** Impact of GPR increase on UHII in four types of spaces at 14:00.

Figure 8. Distribution of outdoor air temperature in residential space at 14:00.

Combined with the urban heat island intensity grading (Table 6), the effects of different GPRs on the four types of space heat intensities vary. Where GPR > 2.5, the urban heat island intensity of the east–west street space is below 3.0, and the urban heat island intensity level is reduced from "strong" to "moderate". For the north–south street space, increasing the GPR mitigates the urban heat island intensity up to 0.90 °C, but the overall intensity level of the space is still in the "strong" category. When the GPR reaches 4.5, the intensity of the urban heat island in the courtyard space and the building overhead space is reduced to the "moderate" level.

Table 6. Urban air temperature urban heat island intensity classification.

UHI Intensity Level	UHII (°C)	Intensity Characteristics
1	UHII ≤ 1	None
2	1 < UHII ≤ 2	Weak
3	2 < UHII ≤ 3	Moderate
4	3 < UHII ≤ 4	Strong
5	UHII > 4	Very strong

The study further analyzes the time-by-time effects of GPR increase on the outdoor air temperature of the four types of spaces. Increasing greenery can reduce the outdoor temperatures of the four types of spaces, and the GPR is increased from 0 to 0.5, and the air temperatures of the four types of spaces are reduced by a maximum of 0.76 °C, 0.69 °C, 0.57 °C, and 0.67 °C, respectively (Figure 9). The GPR is increased from 0.5 to 1.5, and the air temperatures of the four types of spaces are reduced by a maximum of 0.23 °C, 0.12 °C, 0.11 °C, and 0.11 °C, with cooling effects of 0.10 °C or more; the GPR is increased from 1.5 to 2.5, the maximum reductions of the four types of spaces are 0.11 °C, 0.09 °C, 0.08 °C, and 0.10 °C, respectively, i.e., the cooling effect caused by the increase in GPR gradually weakened. The GPR increased from 2.5 to 3.5 and 3.5 to 4.5 in the process of the four types of spaces; the maximum cooling effect of the four types of spaces is less than 0.10 °C.
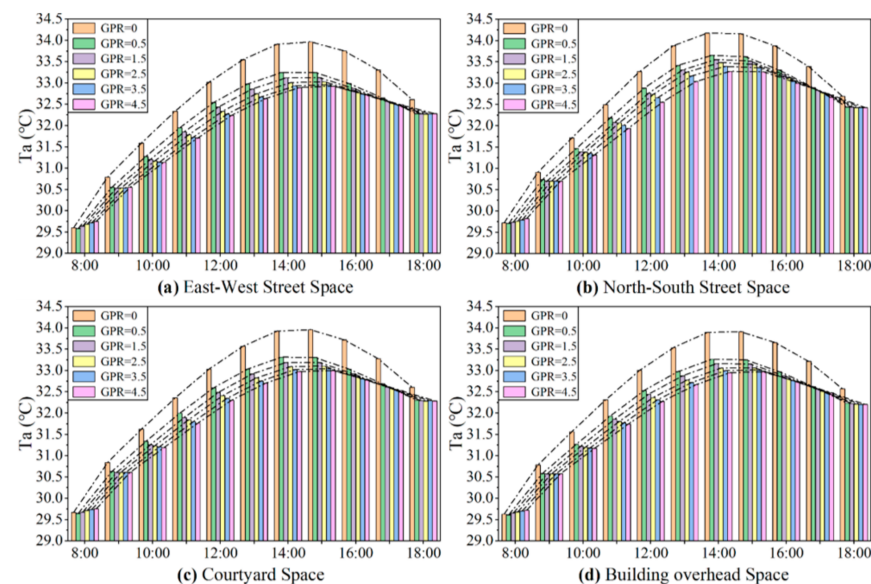

Figure 9. Variation in Ta with the increase in GPR during daytime.

3.1.2. Impact of GPR on Urban Heat Island Intensity during Nighttime

This section analyzes the effect of GPR on the intensity of nighttime urban heat island. Figure 10 illustrates the urban heat island intensity trend with increasing GPR at 22:00. The GPR increases from 0 to 4.5, with the most noticeable increase in the spatial urban heat island intensity for east–west street space at 0.40 °C. The remaining three space urban

heat island intensity increase in essentially the same way, at 0.26 °C, 0.25 °C, and 0.26 °C, respectively. Overall, the nocturnal warming effect due to increased GPR is weak.
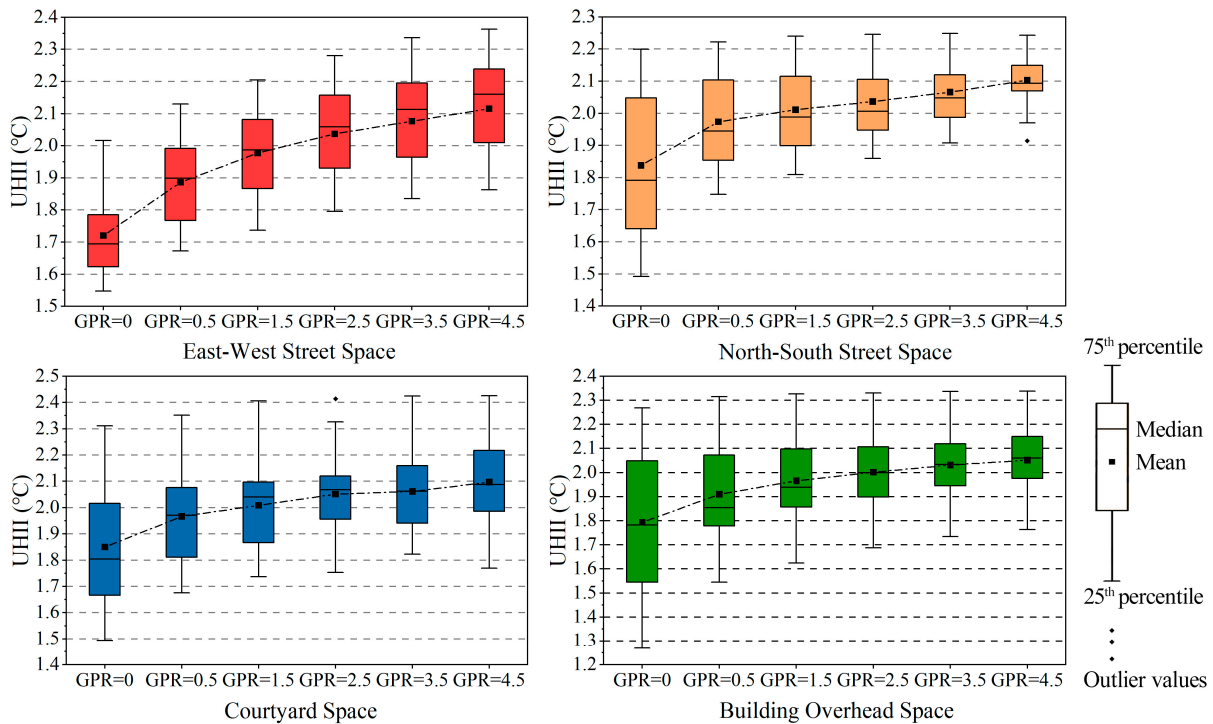

Figure 10. Impact of GPR increase on UHII in four types of spaces at 22:00.

During the nighttime, from 20:00 to 6:00 on the next day, the outdoor air temperature continued to drop (Figure 11). The GPR increase consistently affected outdoor temperatures for all four types of spaces, with outdoor air temperatures increasing with the GPR increase. However, this warming effect diminishes as the GPR increases further.
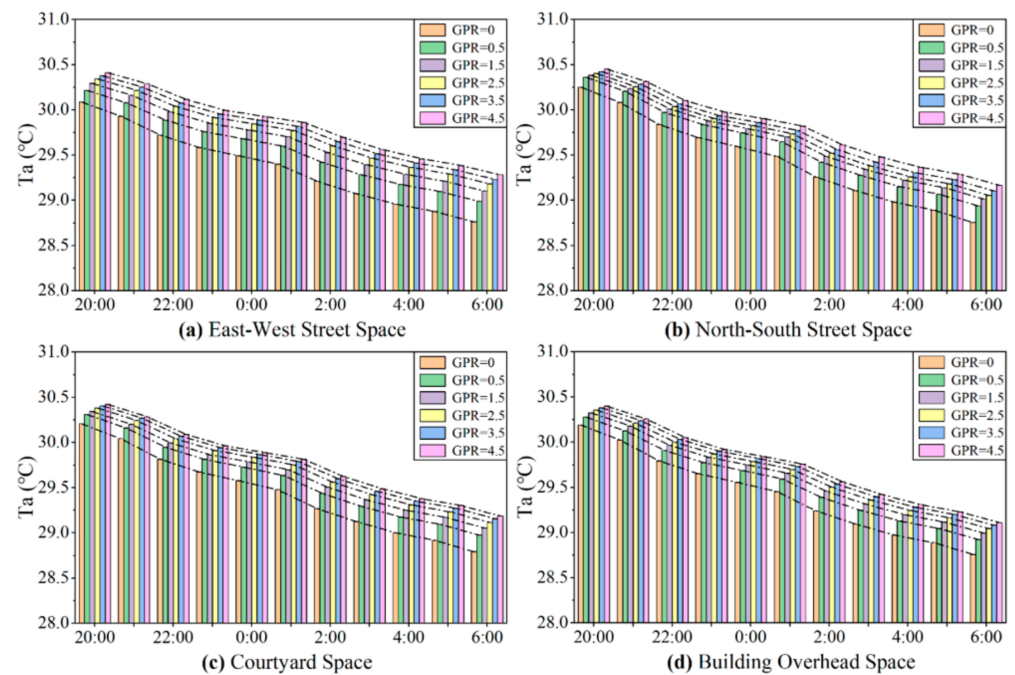

Figure 11. Variation in Ta with the increase in GPR during nighttime.

3.2. Impact of GPR on Outdoor Thermal Comfort in Residential Areas

3.2.1. Impact of GPR on Outdoor Thermal Comfort during Daytime

Figure 12 shows the impact of GPR increase on PET. As the GPR increased from 0 to 4.5, the outdoor PET of four types of spaces had varying degrees of decline during the daytime. The most apparent decline in PET is in the east–west street space, followed by courtyard space, north–south street space, and building overhead space. The PET decreased by 6.61 °C, 6.54 °C, 4.94 °C, and 3.38 °C, respectively. When GPR increased to 0.5, the PET of the building overhead space is reduced to 40.35 °C, and the outdoor thermal comfort transitions from "severe hot" to "hot" according to PET classification in Table 7. When GPR increased to 1.5, the outdoor PET for the north–south street space and the courtyard space is 40.75 °C and 40.86 °C, respectively, and the outdoor thermal comfort is further improved. PET in the east–west street space is obviously improved at GPR above 2.5, with a one-level reduction in human body thermal stress. Notably, the effect of the increase in GPR to improve thermal comfort is not consistently obvious. PET is reduced by 0.38 °C, 0.44 °C, 0.05 °C, and 0.19 °C for the four types of spaces, with the GPR increased from 2.5 to 4.5. Thus, it can be seen that, for courtyard space and building overhead space, the gains in thermal comfort improvement from continued increases in GPR are no longer obvious. Figure 13 shows the outdoor PET distribution at 14:00.
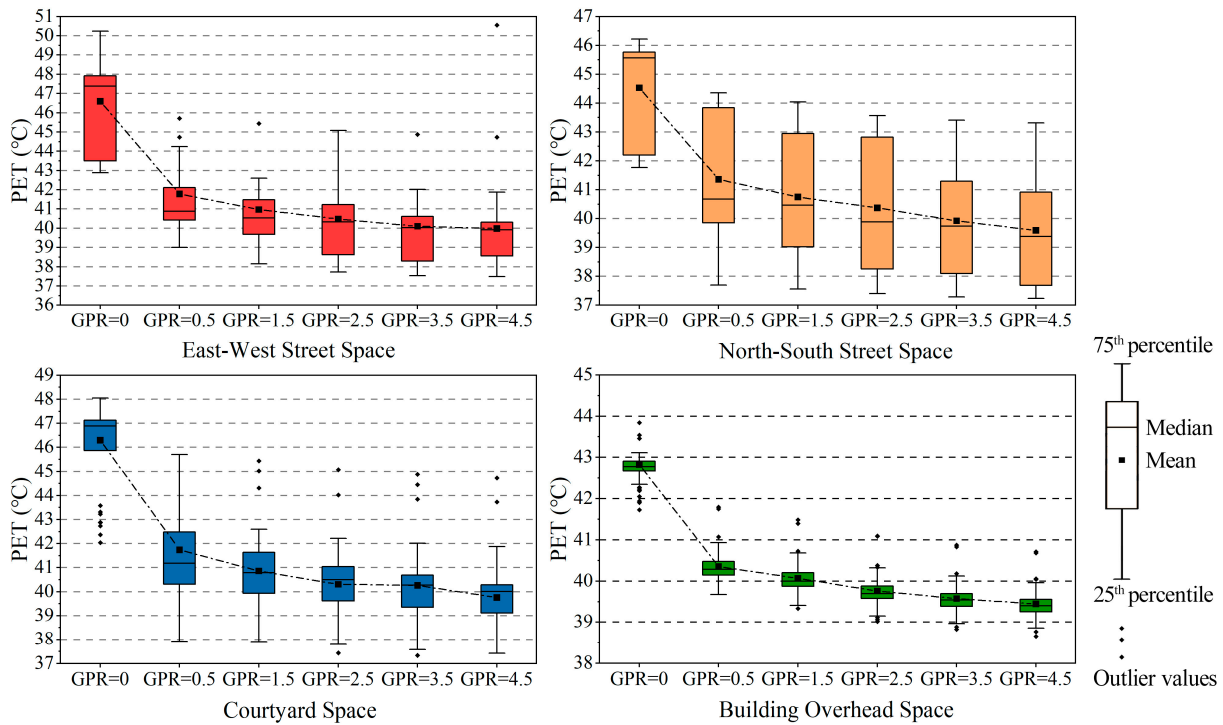

Figure 12. Impact of GPR increase on PET in four types of spaces at 14:00.

Table 7. Thermal Comfort PET Physiological Stress Level Grading Scale for inhabitants [47].

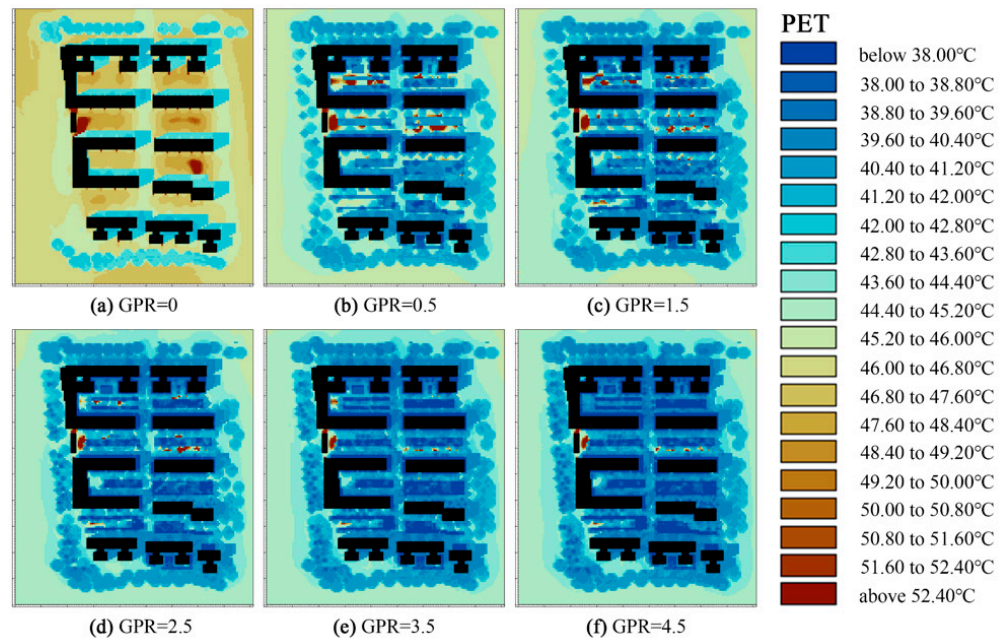| PET	Thermal Sensitivity	Physiological Stress Level
<4 °C	Cold	Strong cold stress
4~8 °C	Cool	Moderate cold stress
8~13 °C	Slightly cool	Slight cold stress
13~23 °C	Comfortable	No thermal stress
23~35 °C	Slightly warm	Slight heat stress
29~35 °C	Warm	Moderate heat stress
35~41 °C	Hot	Strong heat stress
>41 °C	Very hot	Extreme heat stress

Figure 13. Outdoor PET distribution at 14:00.

Figure 14 illustrates the time-by-time trend of outdoor PET with increased GPR for the four types of spaces. For east–west street space, the spacing between the two curves for GPR = 3.5 and 4.5 varied less, indicating a reduced effect of GPR on the time-by-time effect of PET. In the north–south street space, PET at 18:00 changed with increasing GPR, not showing a trend of higher GPR and lower PET. In the courtyard space, the difference in the effect of increased GPR on PET decreases after 17:00. This is due to the gradual weakening of solar radiation, and the effect of GPR on PET decreases.
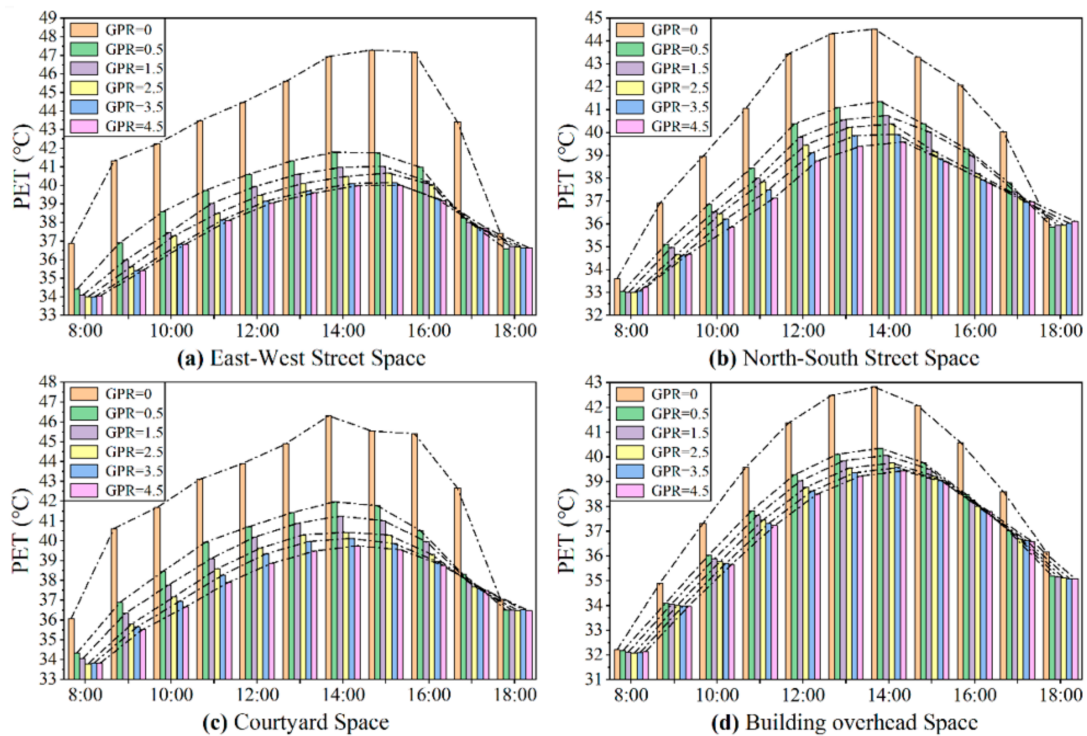

Figure 14. Variation in PET with the increase in GPR during daytime.

3.2.2. Impact of GPR on Outdoor Thermal Comfort during Nighttime

This section demonstrates the impact of GPR on nighttime outdoor thermal comfort. First, the increase in GPR leads to an increase in nighttime PET for all types of spaces in this study (Figure 15). When the GPR was raised from 0 to 4.5, the most noticeable increase in PET was 3.02 °C for the east–west street space, yet the building overhead space only increased by 0.86 °C. Second, the thermal comfort deterioration in the east–west street space was most apparent at night as the GPR continued to increase, and when GPR = 4.5, the outdoor PET in the east–west street space was the highest at 33.57 °C. The effect of GPR on the PET in the courtyard space gradually diminished when GPR > 1.5, as evidenced by an average increment in PET of 0.10 °C.
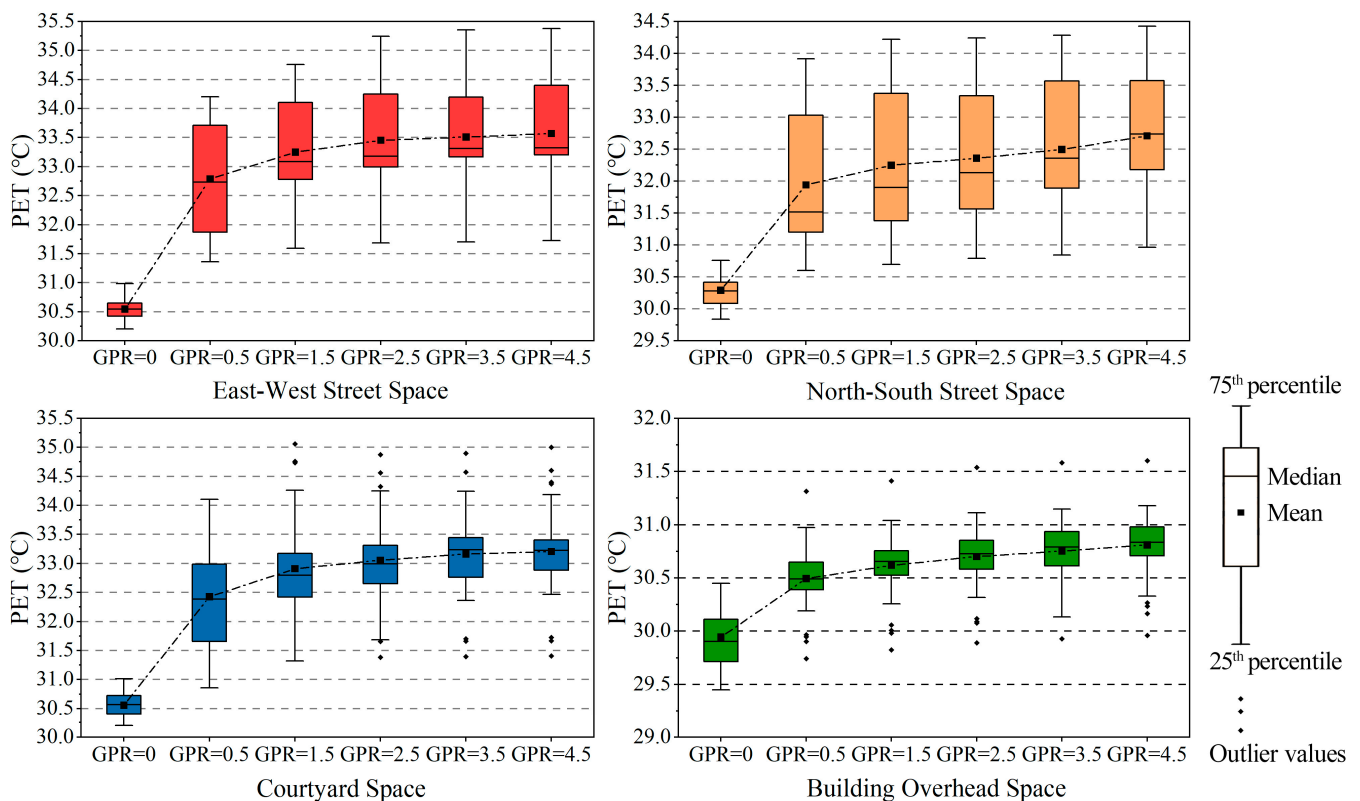

Figure 15. Impact of GPR increase on PET in four types of spaces at 22:00.

Figure 16 shows the night time-by-time variation in outdoor PET with increasing GPR for the four types of spaces. Firstly, nighttime PET shows an overall decreasing trend. Second, among the six GPR scenarios, increasing GPR from 0 to 0.5 has the most noticeable effect on increased outdoor PET in four types of spaces. When GPR is increased from 2.5 to 4.5, the corresponding three survey spacing in Figure 16a is no longer apparent, and when GPR is increased from 3.5 to 4.5, the corresponding curve gap in Figure 16c is also not noticeable. Second, the effect of increasing GPR on the improvement of nighttime outdoor PET in the north–south street space remains evident. The PET in the building overhead space during the nighttime is not as affected by GPR compared with the other three types of spaces obviously.
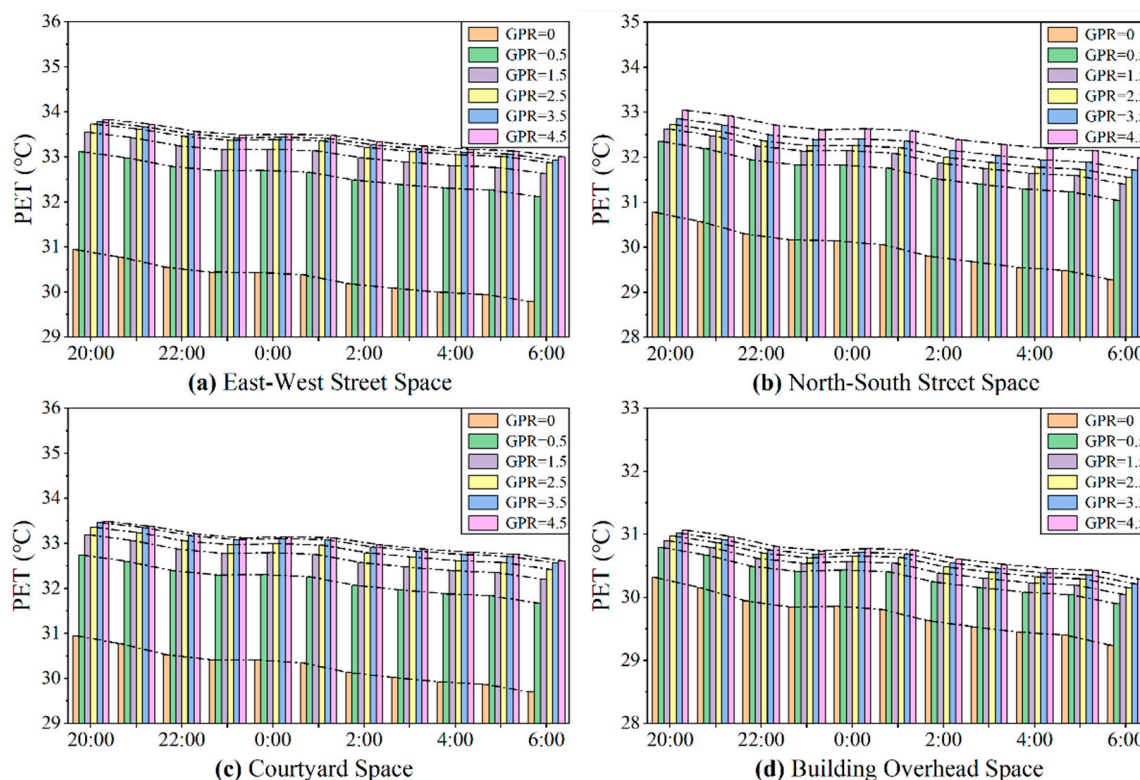
Figure 16. Variation in PET with the increase in GPR during nighttime.

4. Discussion

4.1. Differences in the Effects of GPR on the Intensity of Urban Heat Island of Four Types of Spaces in Residential Areas

The GPR increased from 0 to 4.5, and the daytime urban heat island intensity of the four types of spaces in the residential area decreased by 1.02 °C, 0.95 °C, 0.90 °C, and 0.94 °C, respectively. An increase in GPR represents the increase in the amount of plant greenery in the outdoor space, and as the amount of greenery increases, the overall cooling and humidifying effect of the plants becomes more pronounced [48,49], which effectively reduces air temperature and mitigates the intensity of urban heat islands in settlements. This finding has been confirmed in previous studies [50]. From the analyzed results, it is clear that there are differences in GPR's mitigation of urban heat island intensity for different types of spaces, especially courtyard space. The urban heat island intensity is reduced by only 0.90 °C when the GPR is increased to 4.5, which is due to the more enclosed nature of the courtyard space, resulting in poor air circulation and poor space heat dissipation [51]. Differences in spatial type can have an impact on the effectiveness of GPR in improving daytime urban heat island intensity, which is due to the marked variations in ventilation in different spaces [52], with the north and south street spaces being better ventilated, resulting in an increase in GPR from 3.5 to 4.5 that still reduces the urban heat island intensity by up to 0.12 °C. However, for the remaining three types of spaces, the reduction in urban heat island intensity is less than 0.05 °C.

The GPR increased from 0 to 4.5, and the nighttime urban heat island intensity increased by 0.40 °C, 0.26 °C, 0.25 °C, and 0.26 °C for each of the four types of spaces in the residential area, and a relevant study has confirmed it [53]. This finding means that plants have an "insulating" effect on residential outdoor spaces at night. GPR = 0 represents that there is no planting in the space and the heat received in the space during the daytime will be dissipated at night in the form of longwave radiation [54]. In contrast, with GPR > 0, higher air temperature was observed. Because higher GPR means increased limiting effects of plants on longwave radiation, warm air is trapped under the canopy, with higher air temperature [55].

4.2. Differences in the Effects of GPR on the Thermal Comfort of Four Types of Spaces in Residential Areas

The GPR increased from 0 to 4.5, and the daytime outdoor thermal comfort for the four types of spaces decreased by 7.14 °C (east–west street space), 4.94 °C (north–south street space), 6.56 °C (courtyard space), and 3.38 °C (building overhead space), respectively. Because building overhead space is exposed to less direct sunlight throughout the day, the impact of PET changes due to increased GPR is less apparent [56]. The increase in GPR effectively enhances the cooling and humidifying effect of the plants while increasing the reflection and absorption of solar radiation by the plants, effectively reducing the mean radiant temperature [57], which leads to an obvious decrease in PET. The GPR is less effective in improving thermal comfort in north–south street space than in east–west street space and courtyard space. With limited plant cover and plant greenery, north–south street space is exposed to direct solar radiation for more extended periods throughout the daytime [58]. In addition, a sustained increase in GPR will not constantly improve outdoor thermal comfort. With the increase in the overall green volume of the residential space, the humidification effect of plants is obvious, leading to a further increase in outdoor relative humidity. The conclusion that an increase in relative humidity at high temperatures reduces thermal comfort outdoors has been inferred [59]. The increase in the green volume of plants also impedes the wind speed in the residential area, which is also not conducive to improving thermal comfort [60].

GPR also has a negative effect on nighttime outdoor thermal comfort improvements. The GPR increased from 0 to 4.5, and the thermal comfort index PET for the four space categories increased by 3.02 °C (east–west street space), 2.42 °C (north–south street space), 2.65 °C (courtyard space), and 0.86 °C (building overhead space). While the plant canopy reflects and absorbs solar radiation during the daytime, the plant canopy obstructs long-wave radiation upward from the ground at night [54], resulting in the inability to dissipate heat from space on time and an increase in the mean radiant temperature, thus deteriorating outdoor thermal comfort. The following two points should be focused on for mitigating the impact of greenery on nighttime comfort. The first is to control the volume of greenery, which means keeping the GPR within a specific range. The second is to consider the impact of the greenery layout in residential areas on environmental ventilation because a well-ventilated environment can take away most of the potential heat.

4.3. Proposal of GPR Regulations for Hot-Summer and Cold-Winter Residential Areas Based on Thermal Environment Improvement

In the previous urban planning, two-dimensional indicators such as green space ratio and green coverage ratio were employed to constrain and control the green space in residential areas [61,62]. However, it is not sufficient to consider only from the perspective of two-dimensional indicators. Urban planners have begun to incorporate green plot ratio as one of the evaluation indicators of green space quality to assess the effectiveness of green space from the perspective of three-dimensional spatial green volume. Therefore, this paper studies the effect of the three-dimensional green volume of plants on urban heat island intensity and thermal comfort in urban residential areas. Based on the analyzed results, we provide a reasonable green plot ratio value interval for urban residential spaces according to local conditions, considering the ecological benefits of greenery plants and the economic benefits of environmental construction.

- From the perspective of urban heat island intensity mitigation in urban residential areas, the study recommends that the GPR be set at a value of not less than 3.5 because among the four types of spaces in residential areas, when the GPR is above 3.5, the urban heat island intensity in the east–west street space, the courtyard space, and the building overhead space is below 3.0 °C, with a "moderate" urban heat island intensity.
- From the perspective of thermal comfort improvement in urban residential areas, the study suggests that the GPR should be higher than 1.5 because then the thermal

comfort of the four types of spaces in the residential areas will be reduced from "extreme heat stress" to "strong heat stress". However, it should be noted that the GPR should not be higher than 3.5, because the improvement of outdoor thermal comfort after the GPR is higher than 3.5 is weak, and a very high GPR will deteriorate the outdoor thermal comfort at night to a certain extent. For the mitigation of urban heat island intensity and the optimization of thermal comfort in different types of spaces in residential areas, GPR can be included as a control indicator.

5. Conclusions

This paper investigated the effect of green plot ratio (GPR) on urban heat island and thermal comfort in residential areas. We selected Tong-tai residence as a typical residential area in Changsha based on the research. According to the calculation method of GPR, we constructed several sets of scenarios and conducted simulations to analyze the effect of GPR on the thermal environment of four types of spaces in residential areas. The conclusions of this study are mainly as follows:

- The greenery can obviously improve the outdoor thermal comfort in residential areas. The east–west street space had the most effective PET reduction, with a PET reduction of 7.14 °C, and the building overhead space had the least effective PET reduction, with a PET reduction of 3.38 °C.
- Increasing GPR will not always have a positive effect. When the GPR exceeds 3.5 in the residential area, the mitigation of urban heat island intensity and the improvement of thermal comfort are not obvious. At the same time, with the increase in GPR, outdoor thermal comfort at night deteriorates.
- Combining the analysis of daytime and nighttime, we suggest that the GPR value should be controlled in a specific range, which can facilitate the cooling effect of greenery during the daytime while improving the thermal comfort at night.
- We need to be fully aware of the nocturnal warming effect of plants near the ground. In our research, we have been concerned that a very high GPR leads to some increase in outdoor air temperature at night since energy stored in the ground is released to the outside world in the form of longwave radiation, but the plants in the high GPR scenarios impede this process. Based on this study, we concluded that it is not better to grow more plants. More attention should be paid to the study of the negative impact of greenery on nighttime thermal comfort in subsequent studies, rational plant arrangement, and good ventilation environment creation, all of which should be carefully explored.

In the practical aspect, this paper proposes the recommended values of GPR for urban heat island intensity mitigation and thermal comfort improvement in residential areas. From a theoretical aspect, it complements the existing studies on green space rate and green coverage and further explores the influence of GPR on the thermal environment of urban space. Admittedly, this paper has some limitations for subsequent research. First, due to the diversity of plant species in the living space, to simplify the model, the study temporarily considered five numerically dominant species of trees and one each of grasses and shrubs in the plant modeling. Second, this study is currently only exploring typical summer weather days, and how GPR affects outdoor comfort in residential spaces in winter can be further explored in subsequent studies. Finally, the GPR planning and control indexes proposed in this paper are for the hot-summer and cold-winter climate zone, and whether their values are suitable for other regions needs to be studied further.

The quality and effectiveness of urban green space should be evaluated more in the context of the change from "incremental development" to "quality enhancement and optimization" of urban development and construction. The study analyzes the impact of GPR on urban heat island intensity and thermal comfort in urban residential areas from the perspective of the amount of plant greenery in residential areas, and based on this, the study proposes the planning control values of GPR, which makes up for the current lack of

thermal environment planning indexes in urban residential areas, and provides feasible index suggestions for urban planning practice.

References

1. Ren, Z.; Fu, Y.; Dong, Y.; Zhang, P.; He, X. Rapid urbanization and climate change obviously contribute to worsening urban human thermal comfort: A national 183-city, 26-year study in China. *Urban Clim.* **2022**, *43*, 101154. [CrossRef]
2. Ye, C.; Schroder, P.; Yang, D.; Chen, M.; Cui, C.; Zhuang, L. Toward healthy and liveable cities: A new framework linking public health to urbanization. *Environ. Res. Lett.* **2022**, *17*, 064035. [CrossRef]
3. Wang, Z.; Zhu, P.; Zhou, Y.; Li, M.; Lu, J.; Huang, Y.; Deng, S. Evidence of relieved urban heat island intensity during rapid urbanization through local climate zones. *Urban Clim.* **2023**, *49*, 101537. [CrossRef]
4. Debbage, N.; Shepherd, J.M. The urban heat island effect and city contiguity. *Comput. Environ. Urban Syst.* **2015**, *54*, 181–194. [CrossRef]
5. Leng, H.; Liang, S.; Yuan, Q. Outdoor thermal comfort and adaptive behaviors in the residential public open spaces of winter cities during the marginal season. *Int. J. Biometeorol.* **2020**, *64*, 217–229. [CrossRef]
6. Rui, L.; Buccolieri, R.; Gao, Z.; Gatto, E.; Ding, W. Study of the effect of green quantity and structure on thermal comfort and air quality in an urban-like residential district by ENVI-met modelling. *Build. Simul.* **2019**, *12*, 183–194. [CrossRef]
7. Gidlof-Gunnarsson, A.; Ohrstrom, E. Noise and well-being in urban residential environments: The potential role of perceived availability to nearby green areas. *Landsc. Urban Plan.* **2007**, *83*, 115–126. [CrossRef]
8. Yang, Y.; Zhou, D.; Wang, Y.; Meng, X.; Gu, Z.; Xu, D.; Han, X. Planning method of centralized greening in high-rise residential blocks based on improvement of thermal comfort in summer. *Sustain. Cities Soc.* **2022**, *80*, 103802. [CrossRef]
9. Kubes, J.; Ourednicek, M. Functional types of suburban settlements around two differently sized Czech cities. *Cities* **2022**, *127*, 103742. [CrossRef]
10. Chen, X.; Zhao, P.; Hu, Y.; Ouyang, L.; Zhu, L.; Ni, G. Canopy transpiration and its cooling effect of three urban tree species in a subtropical city-Guangzhou, China. *Urban For. Urban Green.* **2019**, *43*, 126368. [CrossRef]
11. Richards, D.R.; Fung, T.K.; Belcher, R.N.; Edwards, P.J. Differential air temperature cooling performance of urban vegetation types in the tropics. *Urban For. Urban Green.* **2020**, *50*, 126651.
12. Chen, H.; Liu, R.; Zhang, Y. The Impact of Vegetation Canopy on the Outdoor Thermal Environment in Cold Winter and Spring. *Sustainability* **2023**, *15*, 12818. [CrossRef]
13. Zhang, L.; Zhan, Q.; Lan, Y. Effects of the tree distribution and species on outdoor environment conditions in a hot summer and cold winter zone: A case study in Wuhan residential quarters. *Build. Environ.* **2018**, *130*, 27–39. [CrossRef]
14. Yang, Y.; Zhou, D.; Wang, Y.; Ma, D.; Chen, W.; Xu, D.; Zhu, Z. Economical and outdoor thermal comfort analysis of greening in multistory residential areas in Xi'an. *Sustain. Cities Soc.* **2019**, *51*, 101730. [CrossRef]
15. Sabrin, S.; Karimi, M.; Nazari, R. The cooling potential of various vegetation covers in a heat-stressed underserved community in the deep south: Birmingham, Alabama. *Urban Clim.* **2023**, *51*, 101623. [CrossRef]
16. Lai, D.; Liu, Y.; Liao, M.; Yu, B. Effects of different tree layouts on outdoor thermal comfort of green space in summer Shanghai. *Urban Clim.* **2023**, *47*, 101398. [CrossRef]
17. Yang, J.; Zhao, Y.; Zou, Y.; Xia, D.; Lou, S.; Liu, W.; Ji, K. Effects of Tree Species and Layout on the Outdoor Thermal Environment of Squares in Hot-Humid Areas of China. *Buildings* **2022**, *12*, 1867. [CrossRef]
18. Liu, S.; Zhao, J.; Xu, M.; Ahmadian, E. Effects of landscape patterns on the summer microclimate and human comfort in urban squares in China. *Sustain. Cities Soc.* **2021**, *73*, 103099. [CrossRef]
19. Li, H.; Meng, H.; He, R.; Lei, Y.; Guo, Y.; Ernest, A.-A.; Jombach, S.; Tian, G. Analysis of Cooling and Humidification Effects of Different Coverage Types in Small Green Spaces (SGS) in the Context of Urban Homogenization: A Case of HAU Campus Green Spaces in Summer in Zhengzhou, China. *Atmosphere* **2020**, *11*, 862. [CrossRef]

20. Kotharkar, R.; Bagade, A.; Singh, P.R. A systematic approach for urban heat island mitigation strategies in critical local climate zones of an Indian city. *Urban Clim.* **2020**, *34*, 100701.

21. Sayad, B.; Alkama, D.; Ahmad, H.; Baili, J.; Aljahdaly, N.H.; Menni, Y. Nature-based solutions to improve the summer thermal comfort outdoors. *Case Stud. Therm. Eng.* **2021**, *28*, 101399. [CrossRef]

22. Meili, N.; Acero, J.A.; Peleg, N.; Manoli, G.; Burlando, P.; Fatichi, S. Vegetation cover and plant-trait effects on outdoor thermal comfort in a tropical city. *Build. Environ.* **2021**, *195*, 107733. [CrossRef]

23. Huang, Z.; Wu, C.; Teng, M.; Lin, Y. Impacts of Tree Canopy Cover on Microclimate and Human Thermal Comfort in a Shallow Street Canyon in Wuhan, China. *Atmosphere* **2020**, *11*, 588. [CrossRef]

24. Abdulkarim, K.H.; Abd Ghafar, A.; Lai, L.Y.; Said, I. Effects of Vegetation Covers for Outdoor Thermal Improvement: A Case Study at Abubakar Tafawa Balewa University, Bauchi, Nigeria. *Pertanika J. Sci. Technol.* **2021**, *29*, 2125–2147. [CrossRef]

25. Li, Y.; Lin, D.; Zhang, Y.; Song, Z.; Sha, X.; Zhou, S.; Chen, C.; Yu, Z. Quantifying tree canopy coverage threshold of typical residential quarters considering human thermal comfort and heat dynamics under extreme heat. *Build. Environ.* **2023**, *233*, 110100. [CrossRef]

26. Wu, Z.; Kong, F.; Wang, Y.; Sun, R.; Chen, L. The Impact of Greenspace on Thermal Comfort in a Residential Quarter of Beijing, China. *Int. J. Environ. Res. Public Health* **2016**, *13*, 1217. [CrossRef]

27. Chen, H.; Ooka, R.; Harayama, K.; Kato, S.; Li, X.F. Study on outdoor thermal environment of apartment block in Shenzhen, China with coupled simulation of convection, radiation and conduction. *Energy Build.* **2004**, *36*, 1247–1258. [CrossRef]

28. Hong, Z.; Xu, W.; Liu, Y.; Wang, L.; Ou, G.; Lu, N.; Dai, Q. Retrieval of Three-Dimensional Green Volume in Urban Green Space from Multi-Source Remote Sensing Data. *Remote Sens.* **2023**, *15*, 5364. [CrossRef]

29. Ong, B.L. Green plot ratio: An ecological measure for architecture and urban planning. *Landsc. Urban Plan.* **2003**, *63*, 197–211. [CrossRef]

30. *GB 50180-2018*; Urban Residential Planning and Design Standards Building Code. Ministry of Housing and Urban-Rural Development of the People's Republic of China: Beijing, China, 2018.

31. Luo, X.; Yu, C.W.; Zhou, D.; Gu, Z. Challenges and adaptation to urban climate change in China: A viewpoint of urban climate and urban planning. *Indoor Built Environ.* **2019**, *28*, 1157–1161. [CrossRef]

32. Zain, Z.M.; Taib, M.N.; Baki, S.M.S. Hot and humid climate: Prospect for thermal comfort in residential building. *Desalination* **2007**, *209*, 261–268. [CrossRef]

33. Hunan Provincial Department of Housing and Urban-Rural Development. *Design Standard for Green Building in Hunan Province*; China Construction Industry Publishing House: Beijing, China, 2018.

34. *DB32/T 4174-2021*; Standard for Greening of Urban Residential Area and Companies. Jiangsu Provincial Department of Housing and Urban-Rural Development, Jiangsu Provincial Department of Housing and Urban-Rural Development: Nanjing, China, 2021.

35. *DBJ51/168-2021*; Design Standard for Residential Buildings in Sichuan Province. Sichuan Provincial Department of Housing and Urban-Rural Development, Southwest Jiaotong University Publishing House: Chengdu, China, 2021.

36. *SJG 47-2018*; Assessment Standard for Green Building. Shenzhen Municipal Bureau of Housing and Construction, Shenzhen Municipal Bureau of Housing and Construction: Shenzhen, China, 2018.

37. *DGJ 08-2139-2018*; Green Design Standard for Residential Building. Shanghai Municipal Commission of Housing and Urban-Rural Development, Shanghai Municipal Commission of Housing and Urban-Rural Development: Shanghai, China, 2020.

38. *DBJ 13-197-2017*; Design Standard for Green Buildings in Fujian. Fujian Provincial Department of Housing and Urban-Rural Development, Fujian Provincial Department of Housing and Urban-Rural Development: Quanzhou, China, 2018.

39. Chen, D.; Chen, H.W. Using the Köppen classification to quantify climate variation and change: An example for 1901–2010. *Environ. Dev.* **2013**, *6*, 69–79. [CrossRef]

40. Liu, X.; Chen, X.; Shahrestani, M. Optimization of insulation thickness of external walls of residential buildings in hot summer and cold winter zone of China. *Sustainability* **2020**, *12*, 1574. [CrossRef]

41. Liu, X.; Wang, W.; Wang, Z.; Song, J.; Li, K. Simulation Study on Outdoor Wind Environment of Residential Complexes in Hot-Summer and Cold-Winter Climate Zones Based on Entropy-Based TOPSIS Method. *Sustainability* **2023**, *15*, 12480. [CrossRef]

42. Liu, J.; Tang, H.; Zheng, B. Simulation study of summer microclimate in street space of historic conservation areas in China: A case study in Changsha. *Front. Environ. Sci.* **2023**, *11*, 1146801. [CrossRef]

43. Qiu, X.; Kil, S.-H.; Jo, H.-K.; Park, C.; Song, W.; Choi, Y.E. Cooling Effect of Urban Blue and Green Spaces: A Case Study of Changsha, China. *Int. J. Environ. Res. Public Health* **2023**, *20*, 2613. [CrossRef]

44. Xiong, Y.; Zhang, F. Effect of human settlements on urban thermal environment and factor analysis based on multi-source data: A case study of Changsha city. *J. Geogr. Sci.* **2021**, *31*, 819–838. [CrossRef]

45. Chow, W.T.L.; Pope, R.L.; Martin, C.A.; Brazel, A.J. Observing and modeling the nocturnal park cool island of an arid city: Horizontal and vertical impacts. *Theor. Appl. Climatol.* **2011**, *103*, 197–211. [CrossRef]

46. Zhang, S.; Zhang, X.; Niu, D.; Fang, Z.; Chang, H.; Lin, Z. Physiological equivalent temperature-based and universal thermal climate index-based adaptive-rational outdoor thermal comfort models. *Build. Environ.* **2023**, *228*, 109900. [CrossRef]

47. Lin, T.-P.; Matzarakis, A.; Hwang, R.-L. Shading effect on long-term outdoor thermal comfort. *Build. Environ.* **2010**, *45*, 213–221. [CrossRef]

48. Jáuregui, E. Influence of a large urban park on temperature and convective precipitation in a tropical city. *Energy Build.* **1990**, *15*, 457–463. [CrossRef]

49. Cohen, P.; Potchter, O.; Matzarakis, A. Daily and seasonal climatic conditions of green urban open spaces in the Mediterranean climate and their impact on human comfort. *Build. Environ.* **2012**, *51*, 285–295. [CrossRef]

50. Fu, J.; Dupre, K.; Tavares, S.; King, D.; Banhalmi-Zakar, Z. Optimized greenery configuration to mitigate urban heat: A decade systematic review. *Front. Archit. Res.* **2022**, *11*, 466–491. [CrossRef]

51. Forouzandeh, A. Comparative analysis of sol-air temperature in typical open and semi-closed courtyard spaces. *Build. Simul.* **2022**, *15*, 957–973. [CrossRef]

52. Erlwein, S.; Zoelch, T.; Pauleit, S. Regulating the microclimate with urban green in densifiying cities: Joint assessment on two scales. *Build. Environ.* **2021**, *205*, 108233. [CrossRef]

53. Li, Y.; Fan, S.; Li, K.; Zhang, Y.; Kong, L.; Xie, Y.; Dong, L. Large urban parks summertime cool and wet island intensity and its influencing factors in Beijing, China. *Urban For. Urban Green.* **2021**, *65*, 127375. [CrossRef]

54. Chen, G.; Wang, D.; Wang, Q.; Li, Y.; Wang, X.; Hang, J.; Gao, P.; Ou, C.; Wang, K. Scaled outdoor experimental studies of urban thermal environment in street canyon models with various aspect ratios and thermal storage. *Sci. Total Environ.* **2020**, *726*, 138147. [CrossRef]

55. Wujeska-Klause, A.; Pfautsch, S. The Best Urban Trees for Daytime Cooling Leave Nights Slightly Warmer. *Forests* **2020**, *11*, 945. [CrossRef]

56. Weng, J.; Luo, B.; Xiang, H.; Gao, B. Effects of Bottom-Overhead Design Variables on Pedestrian-Level Thermal Comfort during Summertime in Different High-Rise Residential Buildings: A Case Study in Chongqing, China. *Buildings* **2022**, *12*, 265. [CrossRef]

57. Lachapelle, J.A.; Krayenhoff, E.S.; Middel, A.; Coseo, P.; Warland, J. Paper Maximizing the pedestrian radiative cooling benefit per street tree. *Landsc. Urban Plan.* **2023**, *230*, 104608. [CrossRef]

58. Zaki, S.A.; Toh, H.J.; Yakub, F.; Saudi, A.S.M.; Ardila-Rey, J.A.; Muhammad-Sukki, F. Effects of Roadside Trees and Road Orientation on Thermal Environment in a Tropical City. *Sustainability* **2020**, *12*, 1053. [CrossRef]

59. Du, C.; Li, B.; Liu, H.; Li, C. Effect of air humidity on human acceptable thermal environments and evaluation. *Chin. Sci. Bull.-Chin.* **2020**, *65*, 311–324. [CrossRef]

60. Li, J.; Zheng, B.; Ouyang, X.; Chen, X.; Bedra, K.B. Does shrub benefit the thermal comfort at pedestrian height in Singapore? *Sustain. Cities Soc.* **2021**, *75*, 103333. [CrossRef]

61. Zhu, R.; Liu, Y.; Yan, B.; Zhang, X.; Yuan, L.; Wang, Y.; Pan, Y. Effects of district parameters, green space and building density on thermal comfort- a case study of Badaguan District in Qingdao. *Case Stud. Therm. Eng.* **2023**, *42*, 102705. [CrossRef]

62. Luo, Y.; He, J. Evaluating the heat island effect in a planned residential area using planning indicators. *J. Build. Eng.* **2021**, *43*, 102473. [CrossRef]